Title

Chemical signatures of aged Pacific marine air: Mixed layer and free troposphere as measured during PEM-West A

Journal

Journal of Geophysical Research, 101(D1)

ISSN

0148-0227

Authors

Gregory, GL
Bachmeier, AS
Blake, DR
et al.

Publication Date

1996-01-20

DOI

10.1029/95jd00410

JOURNAL OF GEOPHYSICAL RESEARCH, VOL. 101, NO. D1, PAGES 1727–1742, JANUARY 20, 1996

Chemical signatures of aged Pacific marine air: Mixed layer and free troposphere as measured during PEM-West A

G. L. Gregory,[1] A. S. Bachmeier,[2] D. R. Blake,[3] B. G. Heikes,[4] D. C. Thornton,[5] A. R. Bandy,[5] J. D. Bradshaw,[6] and Y. Kondo[7]

Abstract. The Pacific Ocean is one of the few remaining regions of the northern hemisphere that is relatively free of direct anthropogenic emissions. However, long-range transport of air pollutants is beginning to have a significant impact on the atmosphere over the Pacific. In September and October 1991, NASA conducted the Pacific Exploratory Mission-West A expedition to study the atmospheric chemistry and background budgets of key atmospheric trace species. Aircraft sampling centered on the northern Pacific, 0° to 40°N and 115° to 180°E. The paper summarizes the chemical signature of relatively well-aged Pacific marine air (residence time ≥10 days over the ocean). The chemical signatures show that marine air is not always devoid of continental influences. Aged marine air which circulates around the semipermanent subtropical anticyclone located off the Asian continent is influenced by infusion of continental air with anthropogenic emissions. The infusion occurs as the result of Asian outflow swept off the continent behind eastward moving cold fronts. When compared to aged marine air with a more southerly pathway, this infusion results in enhancements in the mixing ratio of many anthropogenic/continental species and typically those with lifetimes of weeks in the free troposphere. Less enhancement is seen for the short-lived species with lifetimes of a few days as infused continental emissions are depleted during transport (about a week) around the semipermanent subtropical high.

Introduction

The Pacific Ocean is one of the few remaining regions of the northern hemisphere that is relatively free of direct anthropogenic emissions. In remote regions of the Pacific some distance from the continents and under selected meteorological conditions, biogeochemical cycles can be studied in relatively unperturbed (limited anthropogenic influence) or background conditions. For example, measurements under downslope conditions at the Mauna Loa Observatory (Hawaii) are being used to address remote Pacific region questions including our understanding of photochemistry in low-NO_x free-tropospheric marine environments [*Ridley and Robinson*, 1992]. However, there is little doubt that long-range transport of air pollutants from Asia and, to a lesser extent, North America is beginning to have a significant impact on the atmosphere with the result that background Pacific marine environments are not so pristine as, for example, a decade ago. In fact, one may state that Pacific background tropospheric air can no longer always be described as natural background air devoid of significant anthropogenic influences.

In September and October 1991, NASA, as part of its Tropospheric Chemistry Program, conducted the Pacific Exploratory Mission (PEM) over the western (West) Pacific to study the atmospheric chemistry and background budgets of key atmospheric trace species, namely, nitrogen, sulfur, and ozone. The field expedition was conducted as part of NASA's Global Tropospheric Experiment (GTE) using the acronym of PEM-West A. PEM-West A aircraft sampling centered on the northern hemisphere western Pacific covering a longitude range of about 115° to 180°E. Meteorological conditions selected for the flight missions provided the opportunity to study chemical budgets under both aged\background marine conditions and Asian continental outflow conditions. PEM-West A objectives are discussed in the overview paper [*Hoell et al.*, this issue]. The expedition revisited the region as PEM-West B in February/March 1994 to study late-winter to early-spring meteorological conditions.

For the meteorological conditions and flight locations of PEM West A, air masses residing over the ocean for periods as brief as 1 day to periods exceeding 10 days were frequently sampled. The focus of this paper is to summarize the chemical signature of relatively well-aged Pacific marine air sampled by the NASA aircraft during PEM-West A. In the analyses, only air (mixed layer and free troposphere) which has resided (based on back trajectory analyses) over the ocean for at least 10 days is considered. The term "marine air" used throughout the paper refers to this class of air. About 20% of approximately 120 aircraft flight hours met this aged condition. The chemical signatures presented herein represent a background against which special case studies (from companion papers) of

[1]Atmospheric Sciences Division, NASA Langley Research Center, Hampton, Virginia.
[2]Lockheed Engineering and Sciences Company, Hampton, Virginia.
[3]Department of Chemistry, University of California at Irvine, Irvine, California.
[4]Center for Atmospheric Chemistry Studies, University of Rhode Island, Narragansett.
[5]Chemistry Department, Drexel University, Philadelphia, Pennsylvania.
[6]School of Earth and Atmospheric Sciences, Georgia Institute of Technology, Atlanta, Georgia.
[7]Solar Terrestrial Environment Laboratory, Nagoya University, Toyokawa, Japan.

Paper number 95JD00410.
0148-0227/96/95JD-00410$05.00

Asian continental outflow, stratospheric intrusion, and typhoon effects can be contrasted. As suggested by the data, the chemical signatures presented do not necessarily represent pristine Pacific marine air but are characteristic of air frequently encountered in the region during the September/October time frame and which would be routinely labeled as aged marine air.

Experiment

The aircraft platform was the NASA Ames Research Center DC-8 four-engine jet. Flight plans and a discussion of their scientific goals are given by *Hoell et al.* [this issue]. Flight plans consisted of combinations of controlled rate of ascent or descent spirals, ramp up or ramp down flight legs, and constant altitude flight legs selected to meet the scientific objectives of each flight. In general, 7- to 8-hour missions were flown covering an altitude range of 300 m to about 13 km above mean sea level (msl). The aircraft operated from four staging areas: California, Japan, Hong Kong, and Guam. The three primary bases of operation (Japan, Hong Kong, and Guam) were selected to meet the conditions of sampling air masses of various ages in terms of having seen emissions directly from the Asian continent. From these staging areas, flights covered a latitude range of about 30°N to the equator. A total of 21 flights were flown. Flights 1–3 from Ames Research Center, California, were instrumentation verification flights. Flights 6–9, 12–13, and 15–17 were site-intensive flights based from Japan, Hong Kong, and Guam, respectively. Ferry flights included (1) flights 4–5 from Ames to Yokota, Japan (via Anchorage, Alaska); (2) flights 10–11 from Japan to Hong Kong (via Okinawa); (3) flight 14 from Hong Kong to Guam; and (4) flights 18–21 from Guam to Ames (via Wake Island and Hawaii). Flight 20 was a Hawaiian Island flight designed in conjunction with surface sampling conducted by NOAA/National Center for Atmospheric Research at the Mauna Loa Observatory. The data discussed herein are from flights 6 to 19 which satisfy meteorological conditions discussed below.

The PEM-West aircraft instrumentation is discussed in the overview paper [*Hoell et al.*, this issue], companion papers which focus on a particular measurement or family of species, or references contained therein. Hoell et al. in their Table 2 list the trace species measured on the aircraft along with sample frequency and limits of detection (LOD). All species listed were considered in our analyses, and results for most species are reported in the tables. However, for our marine classification, some measurements were routinely reported as at LOD. These are not given in our tabular results and include (LODs are given in parentheses) isoprene (3 parts per trillion by volume (pptv)), *N*-hexane (3 pptv), pyruvic acid (10 pptv), oxalic acid (2 pptv), methyl sulfonic acid (1 pptv), phosphate (20 pptv), potassium (17 pptv), magnesium (6 pptv), calcium (14 pptv), aluminum (75 pptv), and vanadium (0.05 pptv).

Meteorology

Numerous PEM meteorological products are available and most are discussed by *Bachmeier et al.* [this issue]. A brief summary of the meteorology as it applies to conditions important to aged marine air is given below and is referenced to the mean winds derived from 12 hourly gridded National Meteorological Center analyses during the PEM-West A time period (Figure 1). Figures 1a through 1d depict the mean surface winds, 700-hPa, 500-hPa, and 300-hPa mean winds, respectively. These mean winds suggest two prominent transport pathways (north and south in the figure) for aged marine air into the PEM-West A study area (shown as a box in the figure). The major synoptic-scale features affecting long-range transport into the study area are (1) migratory cyclones (low pressure) with associated cold fronts, (2) the semistationary subtropical anticyclone (high pressure), and (3) the Intertropical Convergence Zone and tropical cyclones.

During PEM-West A, migratory midlatitude cyclones would frequently form and intensify over China/Mongolia or along the east coast of Asia. As these systems moved eastward, their trailing cold fronts formed the boundary between continental air of midlatitude origin and marine air of either tropical or midlatitude origin. Similar cyclones often formed over the central North Pacific. The mean positions of the cold fronts associated with these cyclones are depicted by the thick lines in the figure, with the southernmost frontal location denoted by the dotted lines.

During this time of year the semipermanent subtropical anticyclone is very evident over the western and central North Pacific, centered near 35°N, 167°E at the surface and near 30°N, 162°E at 500 hPa, as illustrated by "A" in Figures 1a and 1c. This feature is primarily responsible for the north transport pathway of aged marine air. While the 10-day backward trajectories for such air masses indicated no passage over land, infusion of continental air swept off the continent behind the eastward moving fronts did affect the chemical composition of the air. Any scavenging of these anthropogenic/continental emissions by cloudiness or precipitation would be minimized in the stable, subsiding flow around the anticyclone. Aged marine air arriving along the north pathway would, at times, exhibit higher levels of anthropogenic/continental emissions than would be expected for air aged 10 days in the marine environment.

The Intertropical Convergence Zone (ITCZ) was situated near 10°N, the normal September-October position. As a result, easterly trade winds originating from both the northern and the southern hemisphere often entered the southern portion of the study region. These deep tropical easterlies were responsible for the south transport pathway of aged marine air. Because of the general presence of these easterlies across the entire tropical Pacific, it is likely that prior to the 10-day back trajectories, some of the aged marine south air had significantly longer residence time over the Pacific and probably came from a region less populated or industrialized than eastern Asia. Once established, the easterlies would be perturbed by the frequent development of tropical cyclones (commonly referred to as "tropical storms" or "typhoons"). Of the six tropical cyclones which developed during the PEM-West A period, five moved through some portion of the study region).

Database Classifications

PEM-West Classification of Air Masses

For purposes of defining source areas and previous emission history, air masses are classified by several methods: (1) back trajectory analyses, (2) aircraft lidar measurements of O_3 and aerosols, and (3) chemical ratios. For the most part, these classification schemes are discussed in four papers of this issue, and classifications developed in one or more of the papers are used by authors of companion papers for their analyses of chemical budgets, processes, and trends. Below is a brief sum-

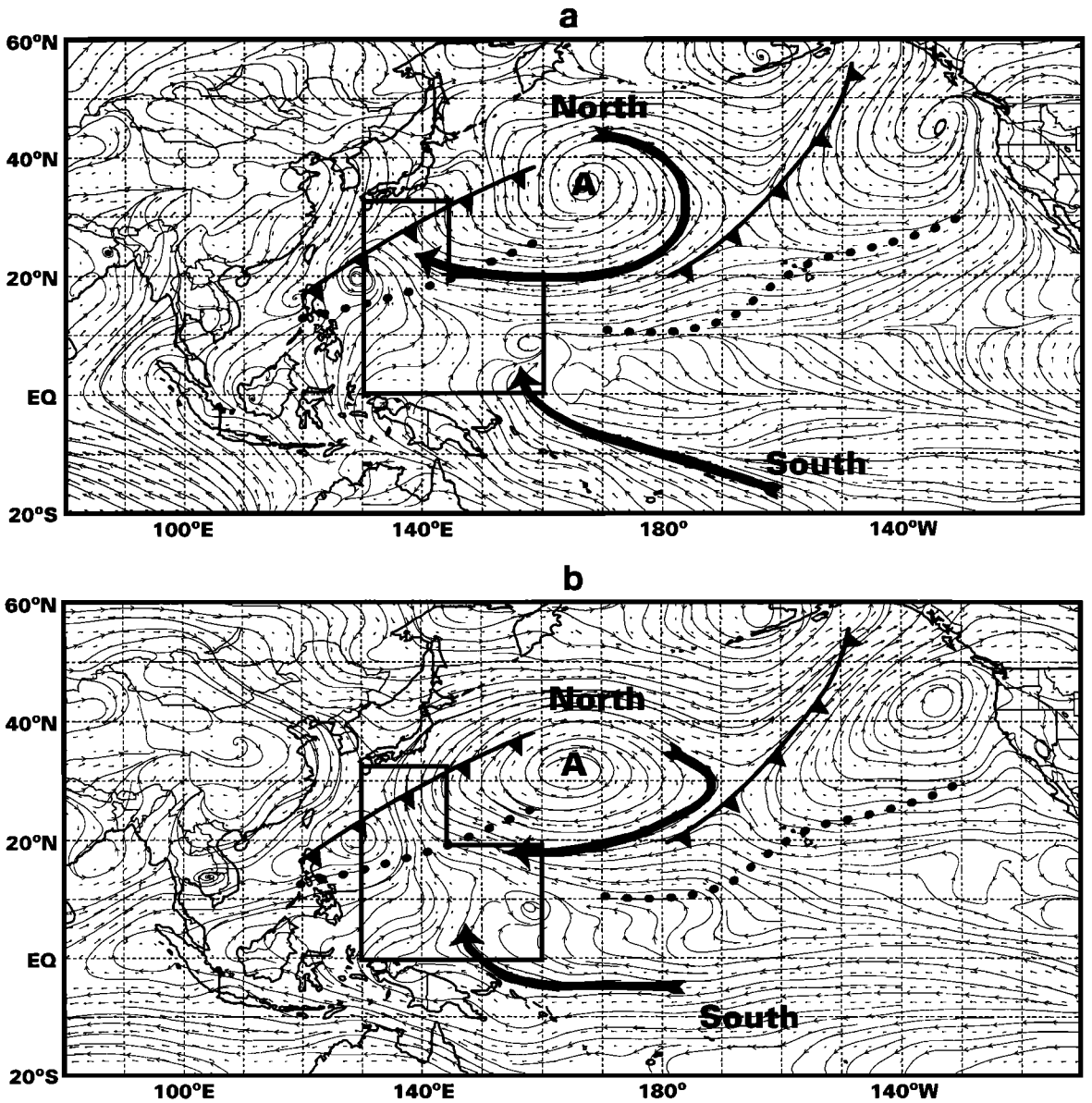

Figure 1. Mean winds for September 16 to October 22, 1991; National Meteorological Center analyses. (a) Surface, (b) 700 hPa, (c) 500 hPa, and (d) 300 hPa. Synoptic features and trajectories for north/south marine data classifications shown in the figures are discussed in the text.

mary of the relationship of the airmass classification papers to each other.

This paper as well as the paper by *Talbot et al.* [this issue] rely on backward trajectory analyses. This paper focuses on the marine environment and defines two classifications of marine-source air (north versus south) which have well-defined (or constrained) trajectories for which air has resided over the ocean for at least 10 days. The paper by *Talbot et al.* [this issue] considers continental-source air (1 to 4 days from the Asian continent) and also constrains trajectories to north and south continental subgroups. *Browell et al.* [this issue] use the lidar O_3 and aerosol altitude profile data measured on the aircraft to classify air into nine groups based upon the relative (i.e., high, low, or equal) signature of O_3 and aerosol as compared to reference profiles established from the lidar data in the PEM study area. These classifications are then related to source areas such as continental, marine, stratospheric, and cloud outflow.

Smyth et al. [this issue] analyze the chemical ratios observed for the various air mass classifications developed in this paper and in the works of *Talbot et al.* [this issue] and *Browell et al.* [this issue]. For the marine data, additional classifications other than our north and south (e.g., equatorial marine and modified marine) are developed by *Smyth et al.* [this issue] using trajectory analyses of *Merrill* [this issue]. *Smyth et al.* [this issue] discuss the merits of chemical ratios as a method of classifying air masses using the chemical ratios calculated for the various classifications developed in this paper and by *Talbot et al.* [this issue] and *Browell et al.* [this issue]. In addition, they interconnect the classification schemes by comparing the results (for the PEM study area) from the three methods.

Marine Classifications Used for Subject Analyses

The databases considered in this paper are classified on the basis of the back trajectory analyses discussed by *Merrill* [this

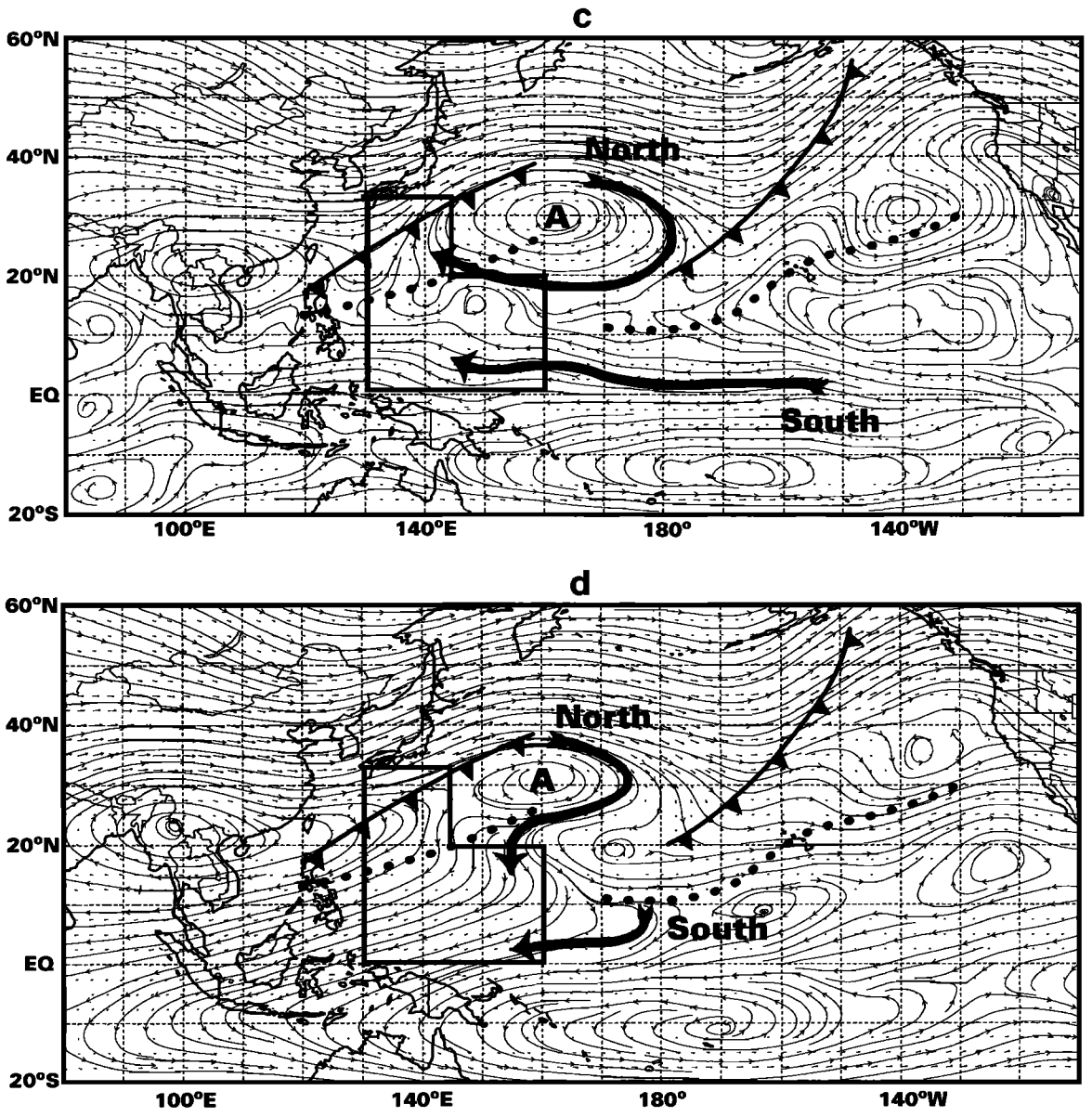

Figure 1. (continued)

issue], which describes the source of the gridded meteorological data, significant assumptions made in the analyses, and the relative reliability of trajectories under the different environmental conditions encountered. Briefly, isentropic back trajectories were calculated postmission for aircraft sampling positions (times) identified as important flight events, e.g., start and end of constant-altitude flight legs, regions of elevated pollution identified from the aircraft data, and regions of expected thermodynamical or dynamical changes identified from aircraft and/or predicted meteorological data. Typically, 15 to 20 trajectories were calculated for each flight. These trajectories represent approximately 60 to 70% of the regions and types of air masses sampled during PEM-West A and include altitudes from within the mixed layer to above 10 km. The goal of each trajectory analyses was to calculate backward trajectories for 10 days at 12-hour intervals. However, as the result of the trajectories leaving the domain (horizontally or vertically) for isentropic analyses, some trajectories end at about 7 or 8 days. Trajectories for mixed layer air generally end after only a few days. The first time step for each trajectory is less than 12 hours and projects the air backward to either 0000 or 1200 UTC. Subsequent time steps are for 12-hour periods ending at either 0000 or 1200 UTC.

Using the trajectory analyses supplied by *Merrill* [this issue], the data from flights 6 to 19 were classified as to measurements of either continental or marine air. Data for which the back trajectories showed the air mass sampled by the aircraft had passed over land within 5 days of the sampling time were classified as "continental." Data for which trajectories showed no land passage for 10 days were labeled as "marine." Islands were treated as land masses. Only data measured during constant-altitude flight are included in the analyses and each constant-altitude flight leg was considered separately in assigning a trajectory path. Thus data from the same flight are found in both databases as some flights sampled both continental and marine air. Where the trajectory did not extend to 10 days and ended, for example, at 8 days, a judgment was made as to whether the air would have passed over land during the addi-

tional 2 days of backward trajectory. This judgment was based upon the location of the air at the last calculated back trajectory location, the direction/magnitude of synoptic winds, and the direction/magnitude of aircraft-measured winds at the flight altitude of interest. When there were insufficient data or some uncertainty as to land passage, the data were excluded from both databases. Included in the continental and marine databases are measurements from seven and nine flights, respectively.

For some analyses, the marine data are further subdivided according to trajectory region and flight altitude. For each subgroup, the chemical data for samples within the group were examined to eliminate any singular data or data from a single flight which were inconsistent with other values for the data grouping. The few exceptions were limited to data measured in the vicinity of Typhoon Mireille (mostly free tropospheric and about 10% of the data initially classified as free tropospheric). For these exceptions the chemical data were inspected, particularly PAN and dimethyl sulfide, as suggested by the results of *Newell et al.* [this issue], and a judgment made as to the representativeness of data in the vicinity of Typhoon Mireille.

Measurement Results

Before discussing the marine results, it is important to place the marine data into perspective in relationship to the continental data. As previously mentioned, the companion paper by *Talbot et al.* [this issue] discusses continental chemical signatures as a function of air mass age (1 to 4 days from the continent); thus only a brief discussion of continental air is presented herein and is limited to observations important to the aged marine air discussions. The databases used for these discussions are those defined above as continental and marine. The continental database (number of samples) may be slightly different than that used by *Talbot et al.* [this issue] which divides continental air into north and south Asian cases; however, results are similar.

In comparing the continental and marine chemical data, it is noted that the continental data show substantial variation in mixing ratios for many species. This is not unexpected since our continental classification does not distinguish between the age of the air and includes air aged 1 to 5 days from the continent. However, after 10 days over the ocean, even the marine data for some species and at times show sizable variations in mixing ratio. The range of variations often includes mixing ratios that are at values typical of clean background air as well as mixing ratios sufficiently high to suggest an anthropogenic influence. For example, for the marine CO data approximately 50% of the observations in the 7- to 9-km altitude band (see Figure 2c, altitude code F) are at mixing ratios <75 parts per billion by volume (ppbv), while 25% are >100 ppbv. Figure 2, in a box-and-whisker format, shows the marine and continental comparisons for O_3, NO_y, CO, PAN, ethane, and acetylene where the data are subdivided into altitude bands based upon the code given in the figure. In the box-and-whisker diagram, the box encompasses 50% of the observations (box boundaries are the upper and lower quartile ranges), the horizontal line (within the box) notes the median of the observations, and the whiskers (vertical lines extending from the box) represent the extremes of the observations. The NO_y data are the Georgia Tech laser-induced fluorescence measurements and were selected since the database included measurements within the mixed layer. The "C" and "M" nomenclature identify the continental and marine data. As previously noted, the marine data include results from nine flights and the continental, seven flights. As discussed below for the marine north and south subsets of data, the marine data of Figure 2 are not completely devoid of continental (anthropogenic) influences. Thus the marine profiles for some species do not always behave as expected for clean marine air. For example, CO increases in mixing ratio with increasing altitude (Figure 2c), and ethane (Figure 2e) and acetylene (Figure 2f) increase above 9 km (altitude code G). These CO and hydrocarbon results suggest continental influences at the higher altitudes. These influences are discussed below as to their importance upon the north marine data group. As it relates to our purposes, the observation of importance from Figure 2 is that the data suggest that marine air, aged at least 10 days over the ocean, can exhibit significant variability in chemical signature and at times the chemical signature suggests that the air is influenced by anthropogenic or continental emissions. The question arises as to the nature of aged marine air and the cause of the variations.

Aged Marine Air: Free Troposphere

The marine data were subdivided according to the trajectories of Figure 1. Marine air in which trajectories showed the air was transported into the sampling region on a path similar to the south case of Figure 1 was grouped as south marine; those with trajectories similar to the north case of Figure 1 were grouped as north marine. Air with marine trajectories of >10 days from regions different than those highlighted as north and south is discussed by *Smyth et al.* [this issue] in their analyses of chemical ratios. Measurements with mixed or questionable (as far as the north/south decision) trajectories were omitted from either grouping. In the analyses of the north and south marine databases, two altitude bands are considered: ≤ 0.5 km altitude representing the mixed layer (ML) and ≥ 3 km altitude representing the free troposphere (FT). For the FT data the north grouping includes data from eight flights (6, 8–10, 14, 16, 18, and 19) and 12 hours of flight and the south grouping, three flights (15, 16, and 21) and 5 hours of flight.

The selected box-and-whisker plots of Figures 3 and 4 illustrate the FT results. The data of Figure 3 are representative of the results for species in which 50% of the north and south observations (the box portion of the box-and-whisker schematic) do not overlap. In our analyses this condition of no overlap is interpreted as the mixing ratios for the specie are statistically different for the data sets. The numbers shown with each diagram reflect the number of measurements incorporated into the box-and-whisker analyses. The data of Figure 4 are representative of species in which the north and south boxes in the box-and-whisker diagrams do overlap. This condition is interpreted in our analyses as showing that there are no significant differences between the data sets. Figure 4b show results from both the Georgia Tech (GT) and the Nagoya University (NU) NO_y instruments aboard the aircraft. The data from the two instruments agree for the south cases (only seven GT samples), while the north results from the two instruments are substantially different. Using GT results, NO_y mixing ratios between the north and the south cases are statistically different. NU results show no difference. As discussed by *Hoell et al.* (this issue), the PEM-West A science team has not completely resolved the differences between the two NO_y measurements.

Table 1 summarizes the results for all species. Given in the

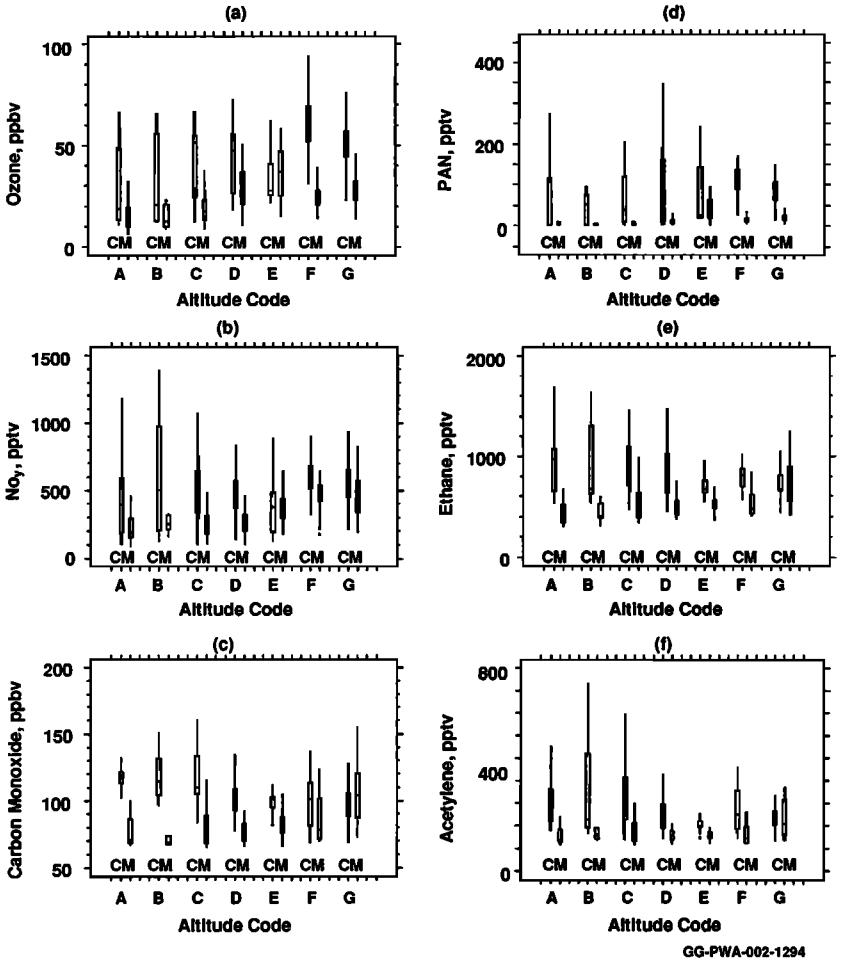

Figure 2. Box-and-whisker diagrams for data classified as continental (C) and marine (M) source air. Continental air has passed over land within 5 days of the sampling time; marine air has not passed over land for at least 10 days. (a) Ozone, (b) NO_y, (c) CO, (d) PAN, (e) ethane, and (f) acetylene. Altitude bands used for the diagrams are referenced to mean sea level as A = <0.5 km, B = 0.5 to 1 km, C = 1 to 3 km, D = 3 to 5 km, E = 5 to 7 km, F = 7 to 9 km, and G = >9 km.

table are median values of the observations, the upper quartile values, and the lower quartile values. A "no data" entry for the south data has been used where measurements include <5 samples. Asterisks identify statistically different results using the above overlapping box criteria (hereinafter noted as box criteria). The box criteria are selected for judging differences in mixing ratios as opposed to averages and confidence intervals because for many species (particularly the north data) there are a few high-valued data, which unduly increases the average. The NO data of the table include only measurements made between 1000 and 1400 LT, i.e., near solar zenith. In examining the results from Table 1, we observe that species with continental or anthropogenic sources and of relatively short lifetimes in the free troposphere (e.g., hours to a few days) tend to show little difference in their mixing ratios whether from the north or the south marine grouping. On the other hand, species with longer tropospheric lifetimes (weeks) show differences (asterisks in Table 1). For example, SO_2 and acetylene (lifetime of about a week), propane and benzene (weeks), ethane (months), CO (lifetime of several months), CO_2 and CH_4 (years), and the freons (almost no tropospheric loss mechanism) show differences, while for example, NO, NO_2, PAN, and ethene (lifetimes of a few days) and propene (few hours) show no differences.

Other comments important to the interpretation of Table 1 are the following:

1. NO_y (particularly the GT measurement) and nitric acid clearly indicate a larger supply of reservoir nitrogen for north marine air as compared to south marine air. A portion of this north/south difference may be attributed to processes not solely dependent on the trajectory classification, some of which are latitude dependent. For example, the increase in stratospheric influences on tropospheric air for the northern regions of the PEM sampling area contributes to the reactive nitrogen reservoir via decomposition of PAN during transport to low altitudes [*Singh et al.*, 1992] as does the frequent occurrence of lightning (hence NO production) over large northern latitude landmasses. Stratospheric exchange is also important to the O_3 budget [*Browell et al.*, this issue]. SO_2 and the sulfur budget are influenced by stratospheric injections as the result of the Pinatubo eruption (three months earlier) [*Thornton et al.*, this issue (a)]. *Browell et al.* [this issue] estimate that for latitudes of 20° to 40°N within the PEM study area, FT air was frequently influenced by stratosphere air and that ~25% of the free

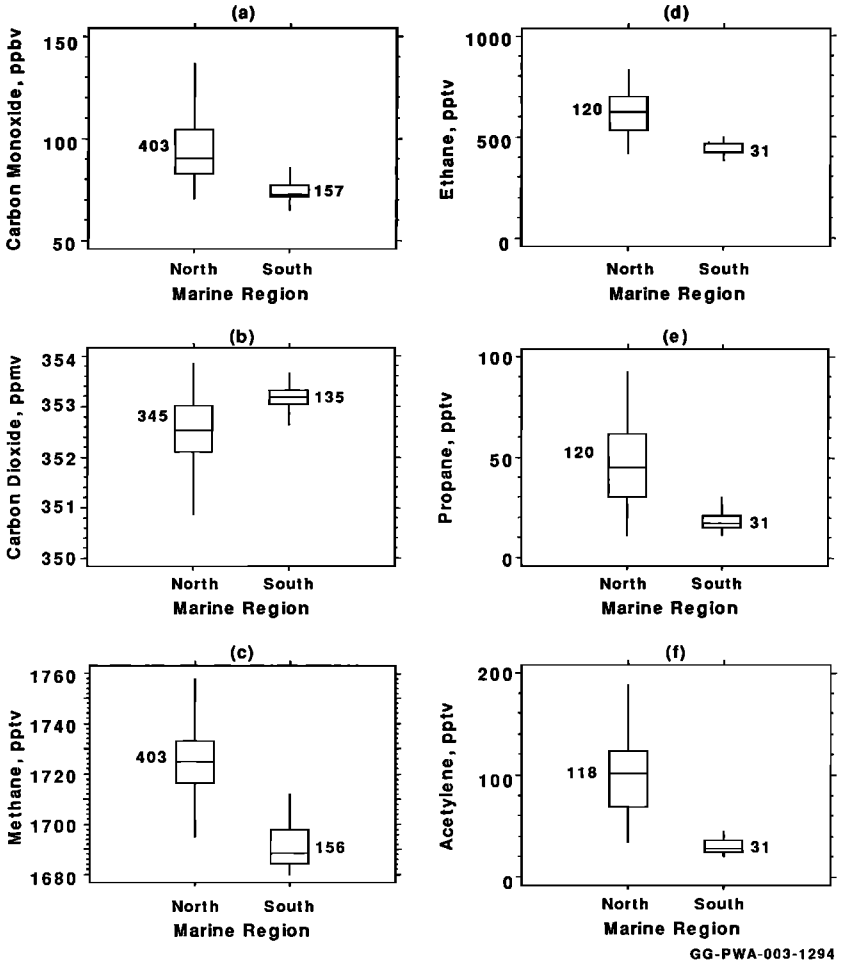

Figure 3. Box-and-whisker diagrams for marine free-tropospheric data classified according to the mean-wind trajectories (north versus south) of Figure 1. Data represent species in which north/south results are interpreted as different. (a) CO, (b) CO_2, (c) CH_4, (d) ethane, (e) propane, and (f) acetylene. The numbers reflect the number of samples included in the analyses.

troposphere was impacted by stratospherically influenced air. At latitudes of 0° to 20°N this percentage decreased to ~6%.

2. Processed species (intermediate species produced via cloud processing, photochemistry, and/or heterogeneous chemistry) in some cases show sizable differences (e.g., nitric and formic acid) between the groupings, while in other cases no differences are observed (e.g., acetic acid and the peroxides). For the first cases the differences (asterisks) of Table 1 may not be entirely the result of the trajectory classification and may also be influenced by the magnitude of previous (during transport) cloud processes, heterogeneous chemistry, and/or wet deposition (rain) which are not considered in the grouping of the data. Similarly for the latter cases, statistical differences which might be present as the result of the trajectory classification may be overshadowed by differences in local production rates (marine environment), production rates during transport (OH chemistry and cloud processing) in the lower troposphere (ML to few kilometers), and loss processes during transport (via wet deposition) on the various flight days. The relatively large interquartile ranges for acetic acid and the peroxides tend to indicate the importance of multiple processes and suggest the need for a database which includes additional observational days (perhaps with sufficient data to include classifications for some of the above processes) before we can be confident that the observed differences (or lack of) for these species are purely the result of trajectory classification. *Heikes et al.* [this issue] discuss peroxide chemistry and observations for the PEM study area.

3. The results shown for the freons, CCl_4, C_2Cl_4, and CH_3Cl_3 (all long-lived species) are mixed. Differences, whether statistically significant or not (based on the box criteria), are relatively small when compared to median FT levels given in the table. For example and for freon 113, the statistical difference shown in the table is based on only a 0.4 pptv delta (north lower quartile of 87.7 minus south upper quartile of 87.3) for a median of about 85 pptv. In many cases, when comparing the mixing ratio ranges for these species within our continental-source classified air and for which the data are restricted to time periods when CO >100 ppbv (significant anthropogenic influence), the interquartile ranges are well within those observed for the marine 10-day classifications of Table 1. In addition and while Asian hot spots [see *Blake et al.*, this issue] do exist, on a relative scale compared to North America and western Europe, the Asian continent as a whole is not a strong source of halocarbon emissions. All the above comments suggest that for these species a larger statistical database with better measurement precision is desirable.

4. Comments similar to the above in terms of a larger da-

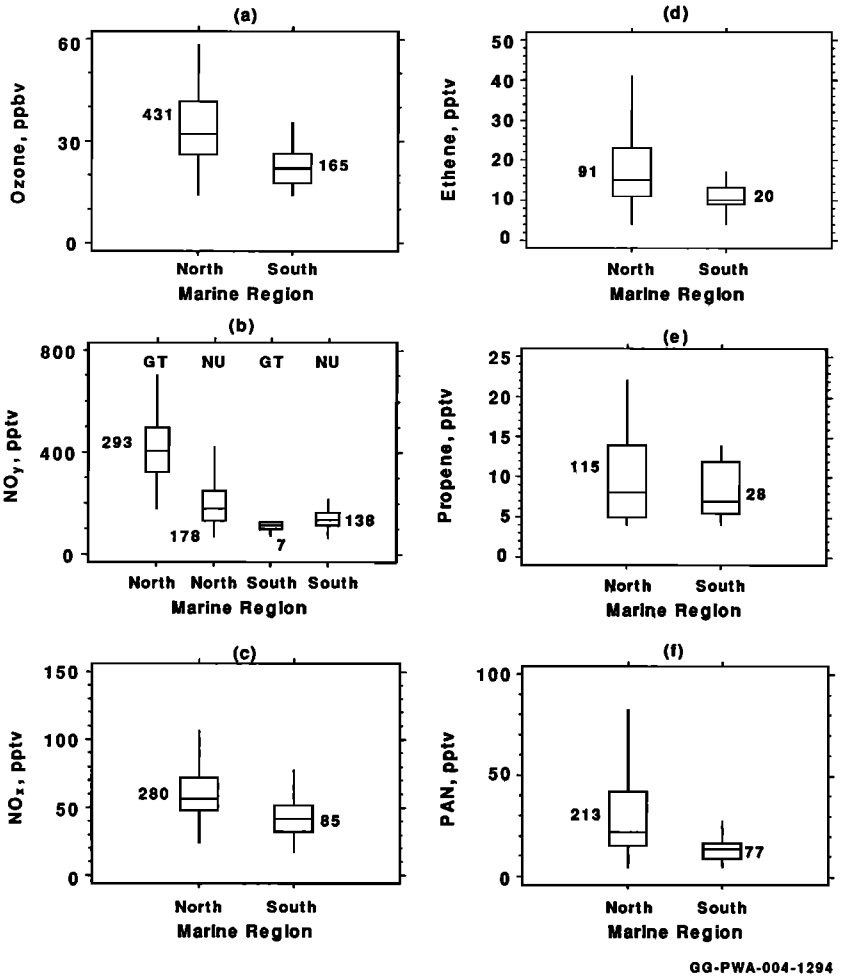

Figure 4. Box-and-whisker diagrams for marine free-tropospheric data classified according to the mean-wind trajectories (north versus south) of Figure 1. Data represent species in which north/south results are interpreted as the same. (a) O_3, (b) NO_y, (c) NO_x, (d) ethene, (e) propene, and (f) PAN. The numbers reflect the number of samples included in the analyses.

tabase apply to both CO_2 and N_2O. The difference shown for CO_2 is barely significant, and while it is consistent with the known vegetative uptake of CO_2 over the continent [*Tans et al.*, 1990] and an eastern tropical Pacific CO_2 source [*Wong et al.*, 1993], a larger database is desirable. On the basis of the above long-lived theory, one expects N_2O to exhibit a statistically significant difference between the data classifications of Table 1 when, in fact, none is shown. However, considering a global FT north/south hemispheric gradient of about 1 pptv for N_2O [*Weiss*, 1981; *Butler et al.*, 1989] compared to its average mixing ratio of about 300 ppbv, a larger statistical database (additional flight days) is probably required to discern such a small difference. In addition, the ocean is a source of N_2O [*Collins et al.*, this issue] and thus, as discussed by *McKeen et al.* [this issue], local production, mixing, and transport may be important in discerning small changes around a large mean. [See *McKeen and Liu*, 1993.]

The results show that the chemical characteristics of free tropospheric aged marine air is significantly different depending on the past trajectory of the air. FT background air (north case, Figure 1) flowing into the western Pacific basin which has circulated around the persistent high-pressure cell located east of the Asian continent (shown at 30°N latitude and 165°E for the 500-hPa level winds of Figure 1c) exhibits enhanced mixing ratios for many anthropogenic/continental trace gases (depleted in the case of CO_2) as compared to background air with trajectories from a more equatorial region (south case, Figure 1). The source of enhancement is believed to be mostly the result of synoptic processes as compared to "localized-" or "event-" oriented processes. Outflow from the Asian continent provides a continual source (at FT altitudes) of continental/anthropogenic emissions which via mixing increases the tropospheric background concentration of selected species. The enhancement occurs mainly for species with lifetimes of weeks and months since any enhancement in the concentrations of the short-lived species (hours to few days) in the continental outflow is greatly diminished as the air circulates around the high-pressure cell (timescale of about 1 week).

The data of Figure 5 provide some information as to the age of the continental emissions infused into the north marine air. Figure 5a shows the propane/ethane ratio (lifetime of weeks/months) for the two marine classifications. Figures 5b and 5c show, respectively, similar plots for the acetylene/CO ratio (lifetime of a week/months) and the ethene/ethane ratio (days/months). On the basis of our overlapping box criteria, the ratios of propane/ethane and acetylene/CO are different for

Table 1. Comparison of Chemical Signatures of North and South Marine Air for the Free Troposphere at Altitudes 3–13 km

	North Marine			South Marine		
		Quartiles			Quartiles	
Specie	Median	Upper	Lower	Median	Upper	Lower
Altitude, km	9.1	10.7	6.5	8.8	9.0	8.7
Air temperature, °C	−23.4	−9.7	−38.6	−22.7	−21.7	−24.2
Dew point, °C	−37.9	−25.2	−43.3	−30.0	−25.1	−36.4
H_2O (Lyman alpha), ppmv	592.1	1068.6	272.3	990.3	1336.9	557.6
Ozone, ppbv	31.9	41.5	26.0	21.9	26.3	17.5
Carbon monoxide,* ppbv	90.4	104.4	82.5	72.6	77.2	71.4
Carbon dioxide,* ppmv	352.5	352.8	352.1	353.2	353.3	353.0
Methane,* ppbv	1724.9	1733.0	1716.7	1688.2	1697.9	1684.4
Nitric oxide (Georgia Tech)	15.3	26.9	8.0	10.3	16.4	8.2
Nitric oxide (Nagoya University)	14.0	24.6	6.7	14.1	18.6	7.1
Nitrogen dioxide	44.2	54.8	32.3	29.7	37.9	19.8
NO_y,* (Georgia Tech)	405.0	498.0	323.0	116.0	128.0	99.0
NO_y (Nagoya University)	178.3	249.4	133.0	137.7	165.5	114.4
PAN	22.1	42.0	15.2	13.9	16.7	8.8
N_2O, ppbv	309.2	309.3	309.0	309.1	309.2	309.0
Sulfur dioxide*	86.0	131.0	70.0	61.0	64.0	51.0
Dimethyl sulfide	6.0	8.0	4.0	5.0	8.0	3.0
Carbon disulfide	1.1	1.8	0.8	0.8	1.0	0.7
Carbonyl sulfide	497.5	505.0	492.0	497.0	501.0	492.0
Hydrogen peroxide	520.0	776.3	280.8	349.8	484.2	237.2
Methyl peroxide	292.0	408.0	195.0	373.5	471.0	314.5
Nitric acid*	65.0	85.0	40.0	7.0	31.0	6.0
Formic acid*	121.0	162.0	90.0	45.0	58.0	36.0
Acetic acid	242.0	344.0	106.0	429.0	596.0	64.0
^7Be, fC/m^3	229.3	404.0	90.0	172.0	172.5	128.0
Toluene	11.5	16.5	7.5	no data	no data	no data
Benzene*	24.0	37.0	15.0	9.0	12.0	6.0
Freon 12*	511.0	514.0	508.0	504.0	505.0	502.0
Freon 11*	276.0	278.0	274.0	272.0	274.0	270.0
Freon 113*	89.1	90.0	87.7	86.6	87.3	86.0
CCl_4	122.0	123.3	120.0	121.0	122.0	120.0
C_2Cl_4*	3.4	4.4	2.8	2.0	2.4	1.9
CH_3CCl_3	154.5	161.0	148.0	150.0	154.0	144.0
Ethane*	621.5	698.0	531.0	428.0	464.0	422.0
Ethene	15.0	23.0	11.0	10.0	13.0	9.0
Propane*	45.2	62.0	30.0	17.0	21.0	15.0
Propane/ethane,* pptv/pptv	0.07	0.10	0.06	0.04	0.05	0.05
Propene	8.0	14 0	5.0	7.0	12.0	5.5
Acetylene*	101.5	123.0	69.0	28.0	36.0	25.0
Acetylene/CO,* pptv/ppbv	1.0	1.2	0.8	0.4	0.4	0.3
I-Butane	9.0	14.0	5.5	LOD	LOD	LOD
N-Butane	10.0	16.0	5.0	no data	no data	no data
I-Pentane	6.0	9.0	4.0	LOD	LOD	LOD
N-Pentane	4.0	6.0	4.0	LOD	LOD	LOD
Butene-1	5.0	7.0	4.0	4.0	5.0	4.0
Butene-1/propane, pptv/pptv	0.10	0.18	0.06	0.25	0.36	0.14
Pentene-1	3.0	4.0	3.0	no data	no data	no data
Chloride	no data	no data	no data	LOD	LOD	LOD
Sulfate	21.0	62.0	13.0	21.0	27.0	19.0
Nitrate	16.0	40.0	8.0	LOD	LOD	LOD
Ammonium	26.0	32.0	25.0	LOD	LOD	LOD
Sodium	99.0	1142.0	98.0	LOD	LOD	LOD

Air has resided over the ocean for at least 10 days (data are given in parts per trillion by volume (pptv) unless noted). For some species, round-off errors result in median and/or quartile values being equal. No data, insufficient number of samples; <5 samples reported as above detection limit. LOD, no data reported, measurements at limit of detection.

*Identifies species which show a statistical difference for the data groupings; that is, interquartile ranges do not overlap; see text discussion of "box criteria."

the north and south marine classifications, while the ethene/ethane ratio (butene/ethane also but not shown in the figure) show no differences. Recognizing that any direct interpretation of chemical ratios for defining air parcel/emission age assumes that atmospheric processing of air is mainly via chemistry as opposed to mixing [see *McKeen et al.*, this issue], we suggest that the data in showing no differences in ratios (to a relatively long-life specie) for species with lifetimes of a few days or less while showing differences for species of lifetimes of a week(s) indicate that the infused emissions at the time of sampling are probably several days aged. In particular for the acetylene/CO ratio (units of pptv/ppbv), ratios <0.5 are generally considered

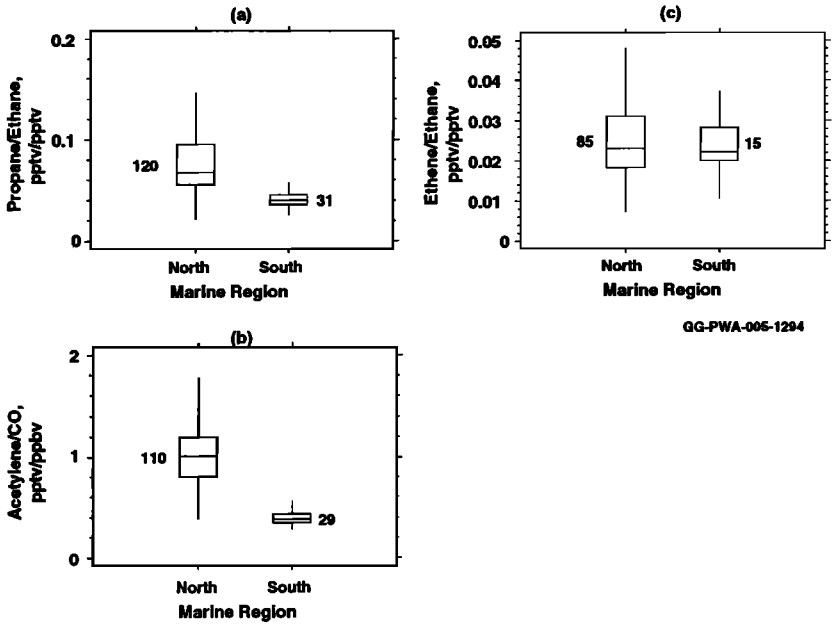

Figure 5. Box-and-whisker diagrams for marine free-tropospheric north and south classification. Data represent specie ratios with different lifetimes. (a) Propane/ethane ratio represents lifetimes of weeks/months; (b) acetylene/CO, ~week/months; (c) ethene/ethane, ~days/months. The numbers reflect the number of samples included in the diagrams.

to be representative of aged air and ratios >1 are indicative of emissions of only a few days age. The median of the ratio for the north marine grouping (Figure 5b) is about 1 (0.4 for south). (For reference, the median of the ratio for our earlier grouped continental data, 1 to 5 days aged, is 1.5 with 50% of the observations having occurred with ratios between 1 and 2.) The paper by *Smyth et al.* [this issue] provides an in-depth discussion of chemical ratios observed in continental and marine air as a function of air mass age. The paper by *McKeen et al.* [this issue] discusses atmospheric mixing processes occurring within PEM-West air and the relative importance of photochemical and mixing processes during transport of air from the Asian continent.

Altitude Observations

Figures 6 and 7 help identify for the north marine case the altitudes at which the effects of Asian continental outflow are most pronounced. The profile data are grouped into 2-km-wide altitude bands starting at 2 km altitude, and box-and-whisker diagrams are plotted at the midpoint of each altitude band. The lower altitude data are grouped into bands of ≤0.5 km altitude and 1 to 2 km, and diagrams are plotted at 0.25 and 1.5 km, respectively. Solid lines connect the median values for the north data; broken lines (panels a only) connect similar altitude groupings for the south data. Altitude bands were selected on the basis of the vertical distribution of the north marine database, and each band includes measurements from at least two flights. The void in data between 1 and 4 km is the result of sparse data in this altitude range. Figure 6 represents the photochemically active/sensitive species O_3, NO_y, and PAN. Both sets of NO_y data are given. Figure 7 represents the sulfur, carbon, and hydrocarbon families with plots of SO_2, CO, ethane, and acetylene. As indicated in the figures and as observed for many (not all) species, maxima exist in the 4- to 8-km altitude range and suggest that Asian continental outflow is most prominent at these altitudes. [See also *Browell et al.*, this issue.] The north data acetylene/CO ratio for the 4- to 8-km altitude bands averages about 1.2, compared to <0.8 for the 10- to 12-km bands and altitude bands below 4 km, and further indicates that air in the 4- to 8-km altitude bands contain, on a relative basis, younger emissions and thus are Asian outflow. Asian outflow in this altitude range is consistent with the meteorological descriptions of *Bachmeier et al.* [this issue] and trajectory analyses of *Merrill* [this issue] which indicate that synoptic conditions favor Asian outflow at these altitudes.

As noted in Figures 7b and 7c, CO and ethane show an increasing gradient with altitude (no maxima in the 4- to 8-km altitude range). While this may be partly due to both the sparsity and the grouping of the data, we believe that the data suggest (most prominent in the ethane data of Figure 7c) that additional anthropogenic/continental outflow is occurring at altitudes as high as 12–14 km. This outflow results in elevated mixing ratios, especially for the longer-lived hydrocarbon species, and tends to mask any maxima that might be present in the 4- to 8-km altitude range. Propane data are similar to the ethane results of Figure 7 and the ratio of propane/ethane (not given in the figure) increases from 0.8 (8- to 10-km band) to ~1.2 (12- to 14-km band and limited data). While our data and analyses do not permit a rigorous assessment, it is highly probable that the anthropogenic/continental emissions present at these higher altitudes are of multiple-continental sources (Asia, Europe, North America) and were advected aloft at a relatively young age and then transported globally into the study area. Hydrocarbons advected into the upper troposphere have relatively long lifetimes compared to those which are transported at lower tropospheric altitudes (e.g., propane lifetime at surface is ~6 days as compared to ~40 days at 10 km [*Greenberg et al.*, 1990]). It is also probable that some of these high-altitude emissions may have been advected aloft (via

clouds) as the air left the Asian coast. While the focus of our analyses is not this upper altitude outflow, it should not be assumed that this outflow is unimportant. For specific days and meteorological conditions (e.g., strong subsidence or storm activity) the higher-altitude outflow could be very important to the chemical signature of air classified in this study as north marine.

The south marine data when subdivided into altitude bands does not contain sufficient samples (some altitude bands include only data from flight 15) to rigorously compare with the north data. However, south data are shown for O_3 and SO_2 ("a" panels and shifted +0.25-km altitude units) and imply that similar enhancements in the 4-km to 8-km altitude range are not prominent in the south data. Where sufficient data are available, enhancements were not observed for most species for the south data.

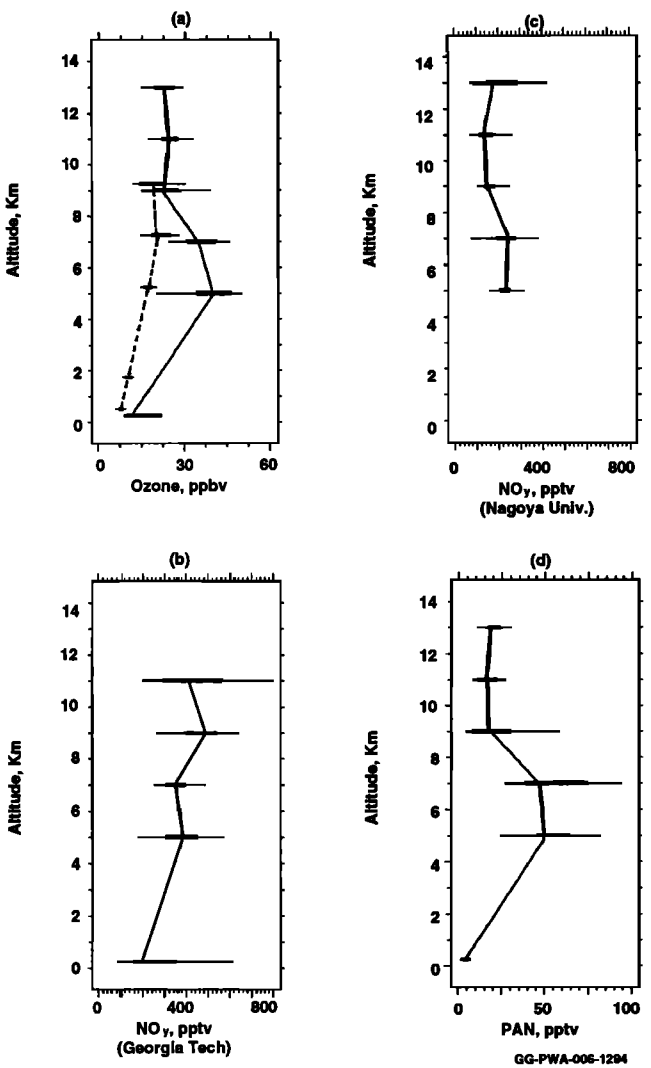

Figure 6. Box-and-whisker diagrams as function of altitude for the north and south marine classification. Data represent the photochemically sensitive species. (a) O_3, (b) Georgia Tech NO_y, (c) Nagoya University NO_y, (d) PAN. Diagrams are plotted at the midpoint of altitude bands discussed in the text and the south data are shifted +0.25-km altitude units for presentation purposes. Solid line connects north median values, broken lines (panel a only), south median values.

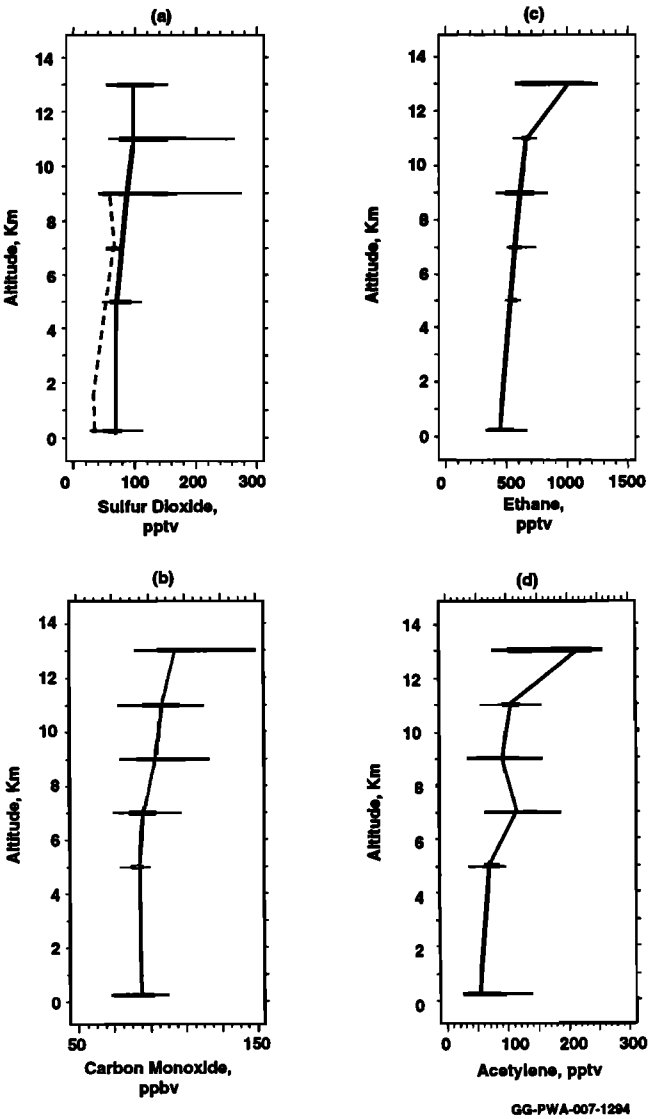

Figure 7. Box-and-whisker diagrams as function of altitude for the north and south marine classification. Data represent chemical families. (a) SO_2 represents the sulfur family; (b) CO represents the carbon family; (c) ethane; and (d) acetylene represents the hydrocarbon family. Diagrams are plotted at the midpoint of altitude bands discussed in the text and the south data are shifted +0.25-km altitude units for presentation purposes. Solid lines connect north median values, broken lines (panel a only), south median values.

Mixed Layer

Table 2 shows ML results for the north and south marine cases. The north data include measurements from two flights and 2.5 hours of flight (early morning and late afternoon), and the south data reflect measurements from only flight 15 and 50 min of flight (midafternoon). Data entries below the broken lines of the table include only three samples for the south data. While we do not consider the results from one or two flights to be necessarily representative of the marine north and south ML in general and noting the time of day differences in the measurements, several features of the data are prominent. Comparison of FT data of Table 1 with ML data of Table 2 clearly shows the ML (north and south) is enhanced in di-

Table 2. Comparison of Chemical Signatures of North and South Marine Air for the Free Troposphere at Altitudes <0.5 km

	North Marine			South Marine		
		Quartiles			Quartiles	
Specie	Median	Upper	Lower	Median	Upper	Lower
Altitude, km	0.4	0.4	0.3	0.3	0.3	0.3
Air temperature,* °C	25.3	25.8	24.9	26.4	26.7	26.2
Dew point,* °C	22.4	22.9	21.7	21.3	21.6	21.0
H_2O (Lyman alpha), ppmv	####	####	####	####	####	####
Ozone,* ppbv	13.1	21.2	11.5	9.0	9.4	8.2
Carbon monoxide,* ppbv	85.5	91.6	70.5	67.8	68.0	67.5
Carbon dioxide,* ppmv	352.5	352.6	352.0	353.4	353.5	353.4
Methane,* ppbv	1713.8	1733.0	1711.0	1672.8	1673.7	1671.8
Nitric oxide,* (Georgia Tech)	3.3	3.4	3.2	4.6	5.1	4.5
Nitric oxide (Nagoya University)	2.3	3.7	0.8	3.0	4.6	1.2
Nitrogen dioxide	17.6	25.3	13.6	15.8	18.4	15.2
NO_y (Georgia Tech)	187.0	350.0	158.0	no data	no data	no data
NO_y (Nagoya University)	####	####	####	####	####	####
PAN	2.0	2.0	2.0	2.0	2.0	2.0
N_2O, ppbv	309.8	310.0	309.4	309.4	309.5	309.2
Sulfur dioxide*	66.0	77.0	49.0	36.0	40.0	35.0
Dimethyl sulfide	54.0	73.0	41.0	47.0	53.0	44.0
Carbon disulfide*	5.7	6.9	1.5	0.6	0.8	0.6
Carbonyl sulfide	500.0	506.0	491.0	498.0	500.0	494.0
Hydrogen peroxide*	1061.1	1229.1	988.2	545.9	647.9	517.9
Methyl peroxide	1491.0	1580.0	1325.0	1826.0	1894.0	1468.0
Nitric acid*	65.0	96.0	37.0	17.0	35.0	13.5
Formic acid*	191.0	242.0	143.0	86.0	142.5	60.0
Acetic acid	173.0	215.0	143.0	176.0	176.0	155.0
	(South Data Below This Line Include Only Three Samples)					
^7Be, fC/m^3	LOD	LOD	LOD	LOD	LOD	LOD
Toluene	13.5	15.0	5.0	no data	no data	no data
Benzene	24.0	30.0	13.0	8.0	9.0	7.0
Freon 12*	509.0	511.0	506.0	501.0	504.0	498.0
Freon 11*	274.0	275.0	269.0	268.0	268.8	266.0
Freon 113*	90.8	92.1	89.7	85.1	85.4	84.9
CCl_4	121.0	123.0	119.0	120.0	121.0	116.0
C_2Cl_4*	4.3	6.0	3.1	1.5	1.6	1.4
CH_3CCl_3	156.5	165.0	150.0	150.0	152.0	148.0
Ethane	434.0	553.0	358.0	360.0	379.0	338.0
Ethene	23.0	30.0	19.0	12.0	24.0	11.0
Propane*	25.2	50.0	13.0	12.0	12.0	11.0
Propane/ethane, pptv/pptv	0.06	0.09	0.04	0.03	0.04	0.03
Propene	14.0	21.5	9.0	no data	no data	no data
Acetylene*	53.5	86.0	33.0	18.0	19.0	16.0
Acetylene/CO,* pptv/ppbv	0.6	0.9	0.5	0.26	0.28	0.24
I-Butane	6.0	7.0	6.0	LOD	LOD	LOD
N-Butane	7.0	10.0	5.0	no data	no data	no data
I-Pentane	4.0	6.0	3.0	LOD	LOD	LOD
N-Pentane	5.5	6.5	3.5	LOD	LOD	LOD
Butene-1	6.0	8.0	4.0	no data	no data	no data
Butene-1/propane, pptv/pptv	0.27	0.38	0.14	no data	no data	no data
Pentene-1	4.0	7.0	4.0	LOD	LOD	LOD
Chloride*	130.0	130.0	100.0	266.0	266.0	182.0
Sulfate*	164.0	164.0	66.0	28.0	11.0	28.0
Nitrate	19.0	19.0	8.7	LOD	LOD	LOD
Ammonium*	122.0	122.0	51.0	40.0	40.0	25.0
Sodium	163.0	297.0	141.0	72.0	72.0	60.0

Air has resided over the ocean for at least 10 days (data are given in pptv unless noted). No data, insufficient number of samples; <3 samples reported as above detection limit; ####, not operational in the mixed layer.

*Identifies species which show a statistical difference for the data groupings; that is, interquartile ranges do not overlap; see text discussion of "box criteria."

methyl sulfide (DMS) and the peroxides. DMS enhancements are of the order of a factor of 8–9; peroxides, a factor of 2–5. Figure 8 plots the results for DMS, methyl peroxide (CH_3OOH), and hydrogen peroxide (H_2O_2) in the format of Figure 6 and is useful for depicting the altitude variance of these species in relationship to mixed layer values. South data are connected with broken lines and are shown in all three panels. While the data of the figure are limited and do not (either data set) include measurements throughout the entire altitude range of interest, several observations are important.

The ocean is a well-documented source of atmospheric DMS [*Bates et al.*, 1987, 1992; *Andreae*, 1990; *Spiro et al.*, 1992]. With a DMS lifetime in the FT of only a few hours, mixing ratios decrease rapidly with altitude, as shown in Figure 8a. Little difference is seen between the north and the south (all altitudes) results.

As shown in Figure 8b, CH_3OOH (as did total organic) exhibits a rapid decrease with altitude, but based on the south data (north data not available), the decrease does not occur until above ~2 km altitude or well above the marine mixing layer. Again, little difference is observed between the north and the south results. H_2O_2 (Figure 8c, north and south) does not show as pronounced a decrease with altitude as CH_3OOH, and north ML values are notably higher than south values. The increase for the peroxides observed at altitudes within several kilometers above the ML and in the ML can be attributed to a combination of cloud processing with transport into the ML, OH radical chemistry, and/or heterogeneous chemistry which occurs within the ML and/or at altitudes within a few kilometers of the top of the ML [e.g., *Bufalini et al.*, 1972; *Levy*, 1973; *Chameides*, 1984; *Adewuyi et al.*, 1984; *Jacob*, 1986; *Heikes*, 1992]. The highly moist, UV enriched, low-NO environment of the tropical marine environment combined with frequent clouds (broken) near the top of the marine mixed layer are conducive to production processes for these species. Whether the higher north ML H_2O_2 values are the result of continental outflow and subsequent processing (clouds, chemistry) and transport into the ML is not evident from our analyses. H_2O_2 differences observed between the north and the south ML may be partly the result of changes in daily production (or loss) rate associated with the different flight days and thus may not solely be the result of the trajectory grouping itself. The ratio of H_2O_2 to CH_3OOH for the north ML is 0.7 compared to 0.3 for the south and may suggest, due to the lower solubility of methyl peroxide in water [*Lind et al.*, 1987], that surface loss and wet deposition processes were larger for the north marine cases. (See *Heikes et al.* [this issue] for a general discussion of peroxide chemistry.)

Figure 9 shows results for nitric acid which are also representative of the altitude structure for acetic and formic acid. (The south data include only ML values due to the lack of

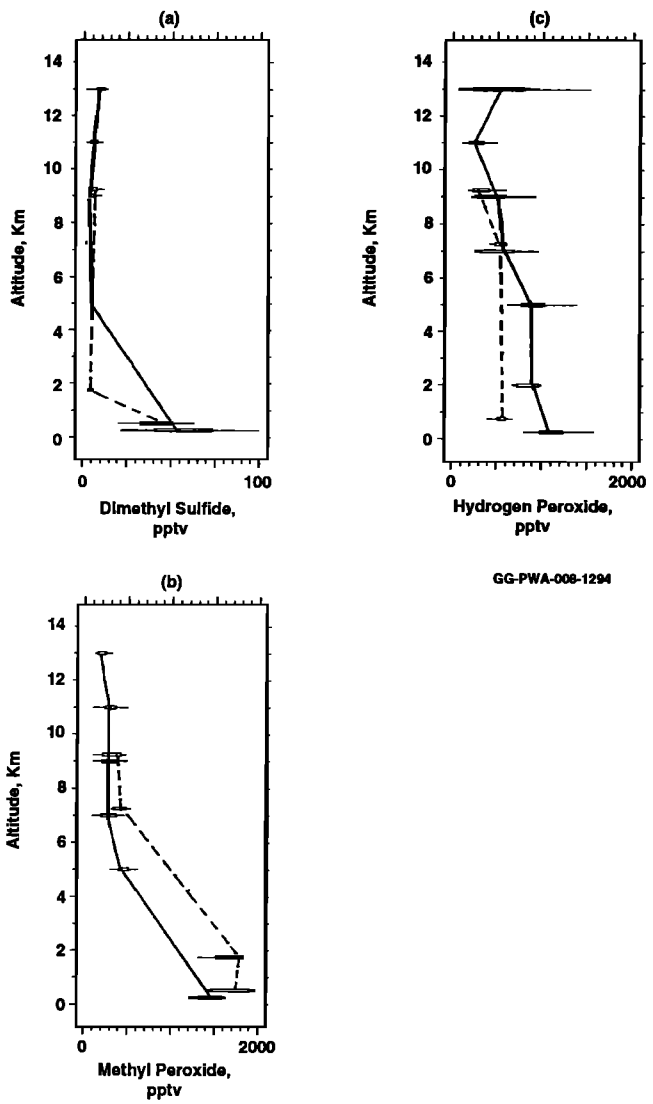

Figure 8. Box-and-whisker diagrams as function of altitude for the north and south marine groupings. Data represent species with a mixing layer and/or lower free-tropospheric (few kilometers) source. (a) Dimethyl sulfide, (b) methyl peroxide, and (c) hydrogen peroxide. Diagrams are plotted at the midpoint of altitude bands discussed in the text and the south data are shifted +0.25-km altitude units for presentation purposes. Solid lines connect north median values, broken lines, south median values.

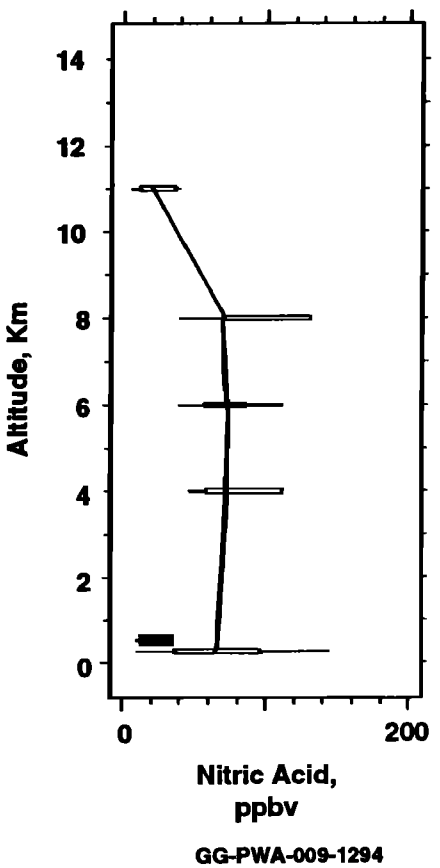

Figure 9. Box-and-whisker diagrams for nitric acid as function of altitude for north marine data. Diagrams are plotted at the midpoint of altitude bands discussed in the text and the solid line connects north median values. South ML data (solid box) are shown for reference.

altitude resolution in the measurements on the one flight day.) For the north data the acids show relatively constant mixing ratios from the ML to about 8 km. Whether this constant gradient with altitude reflects the influence of continental outflow on north marine air cannot be determined from the data. As shown in Figure 9 and Table 2, ML nitric and formic acid mixing ratios are notably higher for the north region than the south, and acetic acid values are similar for both mixing layers.

Other results of Table 2 show statistical differences for some species (asterisks of Table 2). We briefly comment on these observations noting the desire for a larger database from which to rigorously discuss ML observations. First, for those species which showed statistical differences between the north/south FT databases of Table 1, almost all show differences within the ML. The exceptions are NO_y, benzene, and ethane. In the case of NO_y and benzene, no south ML data are available for comparison. On the basis of our box criteria, no statistical difference can be stated for ethane between the north and the south marine ML; however, the median values are consistent with the FT observations as north values are higher, 434 pptv compared to 360 pptv.

The second comment applies to those species which show a statistical difference between the north and the south ML but did not show statistical differences for the FT samples, namely, O_3, NO, CS_2, and H_2O_2. H_2O_2 has already been discussed. For NO the indicated ML difference in Table 2 (GT data only) is only about 1 pptv and is well within the precision of the measurement and the statistical representation of one and two flights for the south and north ML data, respectively.

For O_3 the differences observed within the ML between the north and south data are not the result of changes in ML photochemical loss/production rates associated with the different latitude of the measurements. *Davis et al.* [this issue] calculate the ozone photochemical tendency along the aircraft flight path within the ML; their Table 5 shows values for daily net ozone loss of about 2.5×10^5 molecules/cm^3/s (~0.8 ppbv/24-hour day) for both the ML at 0°–20° and 20°–40°N. These net loss rates are lower than calculated for the remote marine ML over the Atlantic Ocean northeast of Brazil (5°N to 5°S latitude) of ~6 ppb/d [*Anderson et al.*, 1993; *Davis et al.*, 1993]. Assuming similar loss rates of <1 ppbv/d within the marine north and south mixing layers, the 4 ppbv difference (south lower) in O_3 shown in Table 2 is not the result of differences in ozone photochemistry but is probably the result of the higher reservoir FT supply of O_3 for the north marine air (Table 1, 32 versus 22 ppbv). Calculations of *Davis et al.* [this issue] show that for altitudes above the ML, ozone photochemical tendency increases toward more production and less loss as both altitude and north latitude increase.

CS_2 results of Table 2 can be used to illustrate our earlier concern for a larger database to represent ML results. As shown in Table 2, CS_2 is about a factor of 10 (5.7 versus 0.6 pptv) higher in the north ML than in the south ML. No differences were observed for the FT data. However, the CS_2 results for north ML data originated from only two flights. The median value of CS_2 for the two flights were 6.5 and 1.4 pptv. This is within the range observed for the eight flights included in the north FT grouping in which two flights showed medians around 6 pptv, while the other six flight median values were about 1 pptv. For the north data, the ML (flight 8) and FT (flights 6 and 8) sampling in which CS_2 mixing ratios were the highest have back trajectories which suggest strong and persistent continental outflow into the Pacific Ocean relative to other flights. *Thornton et al.* [this issue (b)] uses CS_2 mixing ratios of <1 and >2 pptv to represent clean background marine air and anthropogenically influenced air, respectively.

We conclude that for the marine ML in the PEM-West study area and for the long-lived species (1) the FT is a reservoir source of these gases for both the north and the south marine ML and (2) both mixing layers are net sinks for these gases (via chemistry and/or deposition). Further, we postulate that the tendency for the long-lived species to exhibit higher mixing ratios (CO_2 lower) in the north marine ML as compared to the south ML is the result of the higher reservoir of these species in the north FT (subsequent transport into the ML) as opposed to any sizable differences in the magnitude of deposition and/or chemical loss processes occurring within the respective ML. In arriving at these conclusions, we have assumed that mixing processes between the FT and ML on the experiment days (regardless of latitude) were not drastically different for the reasonably clear flight days. Short-lived species showed no statistical differences between the north and the south ML as none existed in the FT reservoir supply of these species to the ML.

Modeling Results

As part of the PEM-West program, atmospheric chemical modeling was incorporated to aid in the interpretation of the measurement results. The modeling included premission, in the field, and postmission analyses with photochemical three-dimensional and box models. Modeling results are included as both stand-alone papers in this special issue and in papers which focus on trace species or chemical families. In these papers some of the modeling results are processed to provide a simulation of the chemical signature of aged marine air. In many cases it was not possible (due to model mechanics and/or differences in time and spatial scales of the models compared to measurements) to provide simulations that are exactly comparable to measurement products; however, in general, results or trends suggested by the models are consistent with the aged marine observations and conclusions. We comment briefly on results discussed in two of the modeling papers but direct the reader to these and other companion papers for in-depth discussions of models and their application to the aged-marine environment.

Davis et al. [this issue] use a box model to calculate photochemical O_3 tendency (production, loss) along the flight track of the DC-8 aircraft. The calculations incorporated diagnostic modeling techniques which utilized some real-time aircraft measurements of critical O_3-related photochemical parameters and meteorological data to calculate O_3 tendencies along the flight track. In addition, mixing ratios of other key trace species important to O_3 photochemistry are calculated, e.g., OH, nitric acid, and H_2O_2. In general, their results compare favorably to the marine observations. Selecting O_3 as an example, the model shows that the marine ML is a net sink for ozone with a loss rate, when diurnally averaged, of the same magnitude at 0°–20° (south marine) and 20° to 40°N latitude (north). This agrees with our marine observations in which O_3 ML mixing ratios are consistently lower than FT values and provides supporting evidence for our conclusion that the 4 ppbv higher median O_3 for the north ML (compared to south) is not the result of ML photochemistry but is due to a higher north FT reservoir supply of O_3. The model also shows that above the ML, O_3 photochemistry tendency moves toward more production (less loss) as flight altitude and north latitude

increase and thus supports the marine observations of a higher FT reservoir of O_3 for the north data. This move to more O_3 production within the FT results in a model-calculated O_3 column (surface to 12 km altitude) changing from a net loss of about 11×10^{10} (0°–20°N) to a net production of 5×10^{10} molecules/cm^2/s (20°–40°N). The reader is referred to *Davis et al.* [this issue] for additional comparison of modeling and measurement results for other species.

Liu et al. [this issue] use a three-dimensional mesoscale transport/photochemical model to simulate transport and photochemical transformation of trace species during transport from the Asian continent over the Pacific Ocean. Their simulations focus on the September 20 to October 6 portion of the PEM West A study period. In their paper, altitude profiles of trace species simulated by the model are compared with the marine observations of this paper and the continental observations of *Talbot et al.* [this issue]. Agreement was found to be consistent for most species in terms of trends observed between continental and marine air. However, the model underestimates by about a factor of 2 the upper tropospheric transport of Asian boundary layer emissions (e.g., CO and most hydrocarbons). For species like O_3, NO_y, and SO_2, which have a significant stratospheric source, model simulation of trends and mixing ratio differences are in agreement with the measurements. In their paper, box-and-whisker plots as a function of altitude (i.e., similar to our Figure 2) compare model simulations and measurement observations for O_3, NO_y, CO, and acetylene. *Liu et al.* [this issue] conclude that in general, model simulations are in qualitative agreement with the measurements.

Concluding Discussion

The chemical signature for aged marine air which has been over the Pacific Ocean for at least 10 days shows that for some trajectories the air is not always devoid of continental/anthropogenic influences. Analyses of mean winds suggest two distinct pathways for transport of aged marine air into the PEM-West A study area (0°–40°N, 120°–160°E). The major synoptic-scale features important to long-range transport of marine air into the study area are (1) migratory low-pressure cyclones, (2) the semistationary subtropical high-pressure anticyclone, and (3) the Intertropical Convergence Zone and tropical cyclones (storms, typhoons). Marine air (resided over the ocean for at least 10 days) which circulates around the semipermanent subtropical anticyclone located off the Asian continent (e.g., 30°N, 165°E) is influenced by infusion of continental air with anthropogenic emissions. This infusion is the result of persistent Asian continental outflow which is swept off the continent behind cold fronts accompanying eastward moving cyclones. This marine air, classified in the paper as north marine air, shows enhancements in some continental/anthropogenic source species as compared to aged marine air with a more southerly pathway (classified as south marine). The south marine air originates from the eastern and more southerly regions of the Pacific (may have a southern hemisphere component) and is transported into the PEM study region by easterlies.

The enhancement observed for the north marine air occurs mainly for continental/anthropogenic species with lifetimes in the free troposphere (FT) of weeks to months as compared to species with lifetimes of only a few days. Short-lived species are depleted in concentration as the infused continental/anthropogenic emissions are transported (about a week) around the semipermanent subtropical high. The enhancements for the north air occur in the altitude range of a few kilometers to about 8 km, consistent with expected altitudes of outflow from the Asian continent. With the exception of species with sizable oceanic sources (e.g., dimethyl sulfide), differences in mixed layer (ML) concentrations between north and south aged marine air are, for the most part, the result of differences in the FT reservoir supply for the specie rather than major differences in ML chemistry, photochemistry, or surface deposition. For processed or intermediate species like H_2O_2, CH_3OOH, and nitric acid, differences between ML and FT mixing ratios shown for north and south aged marine air may not solely be the result of the trajectory classification but may also depend upon the degree of cloud processing, wet/dry deposition, and heterogenous processing which occurred during transport.

Acknowledgments. The authors express their appreciation to the PEM-West A science team for the many hours of discussion of the aged marine data sets and their many suggestions during preparation of the text. We appreciate the cooperation and helpful suggestion of the NASA Ames Research Center's DC-8 flight, ground, and hangar-support crews in conducting the mission. We acknowledge the support of the various host countries and territories of Japan, Hong Kong, Okinawa, and Guam as well as the hospitality of their citizens. This research was supported by the NASA Global Tropospheric Chemistry Program.

References

Adewuyi, Y. G , S. Y. Cho, R. P. Tsay, and G. R. Carmichael, Importance of formaldehyde in cloud chemistry, *Atmos. Environ.*, *18*, 2413–2420, 1984.

Anderson, B. E., G. L. Gregory, J. D. W. Barrick, J. E. Collins, G. W. Sachse, C. H. Hudgins, J. D. Bradshaw, and S. T. Sandholm, Factors influencing dry season ozone distributions over the tropical South Atlantic, *J. Geophys. Res.*, *98*, 23,491–23,500, 1993.

Anderson, B. E., G. L. Gregory, J. E. Collins, G. W. Sachse, D. Bagwell, and C. H. Hudgins, Airborne observations of the spatial and temporal variability of tropospheric carbon dioxide, *J. Geophys. Res.*, this issue.

Andreae, M. O., Ocean-atmosphere interactions in the global biogeochemical sulfur cycle, *Mar. Chem.*, *30*, 1–19, 1990.

Bachmeier, A. S., R. E. Newell, M. C. Shipham, Y. Zhu, D. R. Blake, and E. V. Browell, PEM-West A: Meteorological overview, *J. Geophys. Res.*, this issue.

Bates, T. S., J. D. Cline, R. H. Gammon, and S. R. Kelly-Hansen, Regional and seasonal variations in the flux of oceanic dimethyl sulfide to the atmosphere, *J. Geophys Res.*, *92*, 2930–2938, 1987.

Bates, T. S., B. K. Lamb, A. Guenther, J. Digon, and R. E. Stoiber, Sulfur emissions to the atmosphere from natural sources, *J. Atmos. Chem.*, *14*, 315–337, 1992.

Blake, D. R., T.-Y. Chen, T. W. Smith Jr., C. J.-L. Wang, O. W. Wingenter, N. J. Blake, F. S. Rowland, and E. W. Mayer, Three-dimensional distribution of nonmethane hydrocarbons and halocarbons over the northwestern Pacific during the 1991 Pacific Exploratory Mission (PEM-West A), *J. Geophys. Res.*, this issue.

Browell, E. V., et al., Large-scale air mass characteristics observed over the western Pacific during the summertime, *J. Geophys. Res.*, this issue.

Bufalini, J. W., B. W. Gay, and K. L. Brubaker, Hydrogen peroxide formation from formaldehyde photooxidation and its presence in urban atmospheres, *Environ. Sci. Technol.*, *6*, 816–821, 1972.

Butler, J. H., J. W. Elkins, T. M. Thompson, and K. B. Egan, Tropospheric and dissolved N_2O of the West Pacific and East Indian Oceans during the El Nino southern oscillation event of 1987, *J. Geophys. Res.*, *94*, 14,865–14,877, 1989.

Chameides, W. L., The photochemistry of a remote marine stratiform cloud, *J. Geophys. Res.*, *89*, 4739–4755, 1984.

Collins, J. E., G. W. Sachse, B. E. Anderson, R. C. Harriss, G. L. Gregory, L. O. Wade, L. G. Burney, and G. F. Hill, Airborne nitrous oxide observations over the western Pacific Ocean: September–October 1991, *J. Geophys. Res.*, this issue.

Davis, D. D., et al., A Photostationary state analysis of the NO_2-NO system based on airborne observations from the subtropical/tropical North and South Atlantic, *J. Geophys. Res.*, *98*, 23,501–23,527, 1993.

Davis, D. D., et al., Assessment of ozone photochemistry in the western North Pacific as inferred from PEM-West A observations during fall 1991, *J. Geophys. Res.*, this issue.

Greenberg, J. P., P. R. Zimmerman, and P. Haagenson, Tropospheric hydrocarbon and CO profiles over the U.S. West Coast and Alaska, *J. Geophy. Res.*, *95*, 14,015–14,026, 1990.

Heikes, B. G., Formaldehyde and hydroperoxides at Mauna Loa Observatory, *J. Geophys. Res.*, 18,001–18,013, 1992.

Heikes, B. G., M. Lee, J. Bradshaw, S. Sandholm, D. D. Davis, W. Chameides, J. Rodriguez, S. Liu, and S. McKeen, Hydrogen peroxide and methylhydroperoxide distributions over the North Pacific in the fall of 1991, *J. Geophys. Res.*, this issue.

Hoell, J. M., D. D. Davis, S. C. Liu, R. Newell, M. Shipham, K. Akimoto, R. J. McNeal, R. J. Bendura, and J. W. Drewry, Pacific Exploratory Mission-West: September–October 1991, *J. Geophys. Res.*, this issue.

Jacob, D. J., Chemistry of OH in remote clouds and its role in the production of formic acid and peroxymonosulfate, *J. Geophys. Res.*, *91*, 9807–9826, 1986.

Levy, H., Photochemistry of minor constituents in the troposphere, *Planet. Space Sci.*, *21*, 575–591, 1973.

Lind, J. A., G. I. Kok, and A. I. Lazrus, Aqueous phase oxidation of sulfur (IV) by hydrogen peroxide, methylhydroperoxide, and peroxyacetic acid, *J. Geophys. Res.*, *92*, 4191–4207, 1987.

Liu, S. C., et al., A model study of tropospheric trace species distributions during PEM-West A, *J. Geophys. Res.*, this issue.

McKeen, S., and S. C. Liu, Hydrocarbon ratios and photochemical history of air masses, *Geophys. Res. Lett.*, *20*, 2363, 1993.

McKeen, S. A., et al., Hydrocarbon ratios during PEM-West A: A model perspective, *J. Geophys. Res.*, this issue.

Merrill, J. T., Trajectory results and interpretation for PEM-West A, *J. Geophys. Res.*, this issue.

Newell, R. E., et al., Atmospheric sampling of Supertyphoon Mireille with the NASA DC-8 aircraft on September 27, 1991, during PEM-West A, *J. Geophys. Res.*, this issue.

Ridley, B. A., and E. Robinson, The Mauna Loa Observatory Photochemistry Experiment, *J. Geophys. Res.*, *97*, 10,285–10,290, 1992.

Singh, H. B., D. Herlth, D. O'Hara, K. Zahnle, J. D. Brawshaw, S. T. Sandholm, P. J. Crutzen, and M. Kanakidou, Relationship of peroxyacetyl nitrate to active and total odd nitrogen at northern high latitudes: Influence of reservoir species on NO_x and O_3, *J. Geophy. Res.*, *97*, 16,523–15,530, 1992.

Smyth, S. J., et al., Comparison of free tropospheric western Pacific air mass classification schemes for the PEM-West A experiment, *J. Geophys. Res.*, this issue.

Spiro, P. A., D. J. Jacob, and J. A. Logan, Global inventory of sulfur emissions with a 1° by 1° resolution, *J. Geophys. Res.*, *97*, 6023–6036, 1992.

Talbot, R. W., et al., Chemical characteristics of continental outflow from Asia to the troposphere over the western Pacific Ocean during September–October 1991: Results from PEM-West A, *J. Geophys. Res.*, this issue.

Tans, P. P., I. Y. Fung, and T. Takahashi, Observational constraints on the global atmospheric CO_2 budget, *Science*, *247*, 1431–1438, 1990.

Thornton, D. C., A. R. Bandy, B. W. Blomquist, D. D. Davis, and R. W. Talbot, Sulfur dioxide as a source of condensation nuclei in the upper troposphere of the Pacific Ocean, *J. Geophys. Res.*, this issue (a).

Thornton, D. C., A. R. Bandy, B. W. Blomquist, and B. E. Anderson, Impact of anthropogenic and biogenic sources and sinks on carbonyl sulfide in the North Pacific troposphere, *J. Geophys. Res.*, this issue (b).

Weiss, R. F., The temporal and spatial distribution of tropospheric nitrous oxide, *J. Geophys. Res.*, *86*, 7185–7195, 1981.

Wong, C. S., Y. H. Chan, J. S. Page, G. E. Smith, and R. D. Bellegay, Changes in equatorial CO_2 flux and new production estimated from CO_2 and nutrient levels in Pacific surface waters during the 1986/87 El Nino, *Tellus.*, *45*(B), 64–79, 1993.

A. S. Bachmeier, Lockheed Engineering and Sciences Company, Hampton, VA 23665-5225.

A. R. Bandy and D. C. Thornton, Chemistry Department, Drexel University, Philadelphia, PA 19104.

D. R. Blake, Department of Chemistry, University of California at Irvine, Irvine, CA 92717.

J. D. Bradshaw, School of Earth and Atmospheric Sciences, Georgia Institute of Technology, Atlanta, GA 30332-0340.

G. L. Gregory, Atmospheric Sciences Division, NASA Langley Research Center, Hampton, VA 23681-001.

B. G. Heikes, Center for Atmospheric Chemistry Studies, University of Rhode Island, Narragansett, RI 02882.

Y. Kondo, Solar Terrestrial Environment Laboratory, Nagoya University, Toyokawa, Japan.

(Received December 29, 1993; revised December 19, 1994; accepted January 20, 1995.)